

FEATURED PAPERS

Molecular assessment of rejection and injury in lung transplant biopsies



Kieran M. Halloran, MD, MSc,^a Michael D. Parkes, MSc,^b Jessica Chang, BSc,^b Irina L. Timofte, MD,^c Gregory I. Snell, MD,^d Glen P. Westall, MD, PhD,^d Ramsey Hachem, MD,^e Daniel Kreisel, MD, PhD,^e Elbert Trulock, MD,^e Antoine Roux, MD, PhD,^f Stephen Juvet, MD, PhD,^g Shaf Keshavjee, MD, MSc,^g Peter Jaksch, MD,^h Walter Klepetko, MD,^h and Philip F. Halloran, MD, PhD^{a,b}

From the ^aDepartment of Medicine, University of Alberta, Edmonton, Alberta, Canada; ^bAlberta Transplant Applied Genomics Center, Edmonton, Alberta, Canada; ^cDivision of Pulmonary and Critical Care, Department of Medicine, University of Maryland at Baltimore, Baltimore, Maryland, USA; ^dLung Transplant Service, Alfred Hospital, Monash University, Melbourne, Australia; ^eDivision of Pulmonary and Critical Care Medicine, Washington University School of Medicine, St. Louis, Missouri, USA; ^fService de Pneumologie, Hôpital Foch, Suresnes, France; ^gDepartment of Medicine University Health Network, Toronto, Ontario, Canada; and the ^hDepartment of Thoracic Surgery, Medical University of Vienna, Vienna, Austria.

KEYWORDS:

microarray;
antibody-mediated
rejection;
T-cell-mediated
rejection;
surfactant;
gene expression

BACKGROUND: Improved understanding of lung transplant disease states is essential because failure rates are high, often due to chronic lung allograft dysfunction. However, histologic assessment of lung transplant transbronchial biopsies (TBBs) is difficult and often uninterpretable even with 10 pieces.

METHODS: We prospectively studied whether microarray assessment of single TBB pieces could identify disease states and reduce the amount of tissue required for diagnosis. By following strategies successful for heart transplants, we used expression of rejection-associated transcripts (annotated in kidney transplant biopsies) in unsupervised machine learning to identify disease states.

RESULTS: All 242 single-piece TBBs produced reliable transcript measurements. Paired TBB pieces available from 12 patients showed significant similarity but also showed some sampling variance. Alveolar content, as estimated by surfactant transcript expression, was a source of sampling variance. To offset sampling variation, for analysis, we selected 152 single-piece TBBs with high surfactant transcripts. Unsupervised archetypal analysis identified 4 idealized phenotypes (archetypes) and scored biopsies for their similarity to each: normal; T-cell-mediated rejection (TCMR; T-cell transcripts); antibody-mediated rejection (ABMR)-like (endothelial transcripts); and injury (macrophage transcripts). Molecular TCMR correlated with histologic TCMR. The relationship of molecular scores to histologic ABMR could not be assessed because of the paucity of ABMR in this population.

CONCLUSIONS: Molecular assessment of single-piece TBBs can be used to classify lung transplant biopsies and correlated with rejection histology. Two or 3 pieces for each TBB will probably be needed to offset sampling variance.

J Heart Lung Transplant 2019;38:504–513

© 2019 International Society for Heart and Lung Transplantation. All rights reserved.

Reprint requests: Philip F. Halloran, MD, PhD, Alberta Transplant Applied Genomics Centre, #250 Heritage Medical Research Centre, University of Alberta, Edmonton, AB T6G 2S2, Canada. Telephone: 780-492-6160. Fax: 780-407-7450.

E-mail address: phallora@ualberta.ca

See Related Editorial, page 514

Lung transplantation plays a major role in management of end-stage lung disease, but outcomes are worse when compared with other organ transplants,^{1,2} with significant graft loss due to the poorly understood syndrome of chronic lung allograft dysfunction (CLAD). The extent to which T-cell-mediated rejection (TCMR, also known as acute cellular rejection) and antibody-mediated rejection (ABMR) contribute to CLAD is not known. The standard of care (SOC) for diagnosing lung rejection is the transbronchial biopsy (TBB) interpreted using International Society for Heart and Lung Transplantation (ISHLT) guidelines.³ The key lesions are perivascular mononuclear cell infiltrates or acute cellular rejection (ACR)^{4,5} (A-grade) and lymphocytic bronchiolitis^{6–8} (B-grade), both likely reflecting TCMR, and obliterative bronchiolitis (C-grade). The LARGO study of TBBs showed that sub-optimal sampling was common and interobserver agreement was poor.^{9–12} The situation for ABMR is even more problematic: the histologic features are non-specific,^{9,13} and clinical ABMR assessment includes factors unrelated to histology.¹⁴ The LARGO investigators concluded that new tools are needed for diagnosing lung transplant rejection.

An emerging alternative to histology is molecular diagnostics.¹⁵ In kidney and heart transplants, a microarray-based diagnostic system (Molecular Microscope® Diagnostic System, or MMDx) has been developed to detect TCMR and ABMR^{16–20} with high technical reproducibility while requiring less tissue. For heart transplants, we used unsupervised machine learning to discover phenotypes based on rejection-associated transcripts (RATs) shared between kidney and heart transplants.^{20–23} This distinguished 4 extreme phenotypes (“archetypes”) and scored biopsies for their similarity to each²⁴: S1_{normal} (absence of inflammation/rejection); S2_{TCMR} (effector T-cell transcripts); S3_{ABMR} (mainly endothelial transcripts); and S4_{injury} (macrophage transcripts).

The present prospective observational study (INTERLUNG ClinicalTrials.gov: [NCT02812290](https://clinicaltrials.gov/ct2/show/study?term=NCT02812290)) adapted the strategy developed for heart biopsies to single-piece lung transplant TBBs (a restriction imposed by institutional review boards [IRBs]). The research plan is outlined in [Figure 1](#). Our goals were to use a discovery-based approach to determine whether TBB pieces can be analyzed by microarrays, to use unsupervised analysis to identify rejection and injury in TBBs, and to relate these findings to histologic diagnoses and donor-specific antibody (DSA) status.

Methods

Population

We prospectively enrolled consenting adult lung transplant recipients from 7 centers (refer to Table S1 in the Supplementary Material available online at www.jhltonline.org). We collected indication biopsies (i.e., clinician concern), protocol biopsies, and follow-up biopsies, collected as per local SOC (see Methods for clinical diagnostics in the Supplementary Material online).

Lung biopsies

TBBs were performed in an accessible lobe as per SOC at participating institutions, with up to 10 TBB pieces collected per patient,

depending on safety and tolerance. One TBB piece was stabilized in RNAlater for microarray analysis (see Methods in Supplementary Material online), and all other pieces were sent for SOC histologic assessment. Mucosal biopsies from the second bronchial bifurcation (2BMB) were performed in a subset of cases to define differentially expressed genes in TBBs. Biopsies were processed with microarrays and the data were normalized, as described elsewhere.^{20,24} The workflow is summarized in Figure S2 (online).

Rejection-associated transcript and pathogenesis-based transcript sets and pathway analysis

Rejection-associated transcripts (RATs), previously identified using published algorithms,²⁰ are the 200 probe sets associated with each of 3 classes of rejection in kidney transplants: all histologic rejection^{23,25} (all-rejection-RATs); TCMR¹⁷ (TCMR-RATs); or ABMR¹⁶ (ABMR-RATs). The union of the top 200 probe sets from each comparison yielded 453 RAT probe sets (260 unique genes), which were used for unsupervised analyses.

Pathogenesis-based transcript sets (PBTs; <https://www.ualberta.ca/medicine/institutes-centres-groups/atacg/research/gene-lists/>) are sets of transcripts derived in experimental animal models, cell lines, or human biopsies for guidance and interpretation of pathogenic processes (see Methods online).

Statistics

Data analyses were performed using Bioconductor version 3.6 and R version 3.4.2. Top genes differentially expressed in TBBs vs 2BMBs were identified by comparing mean probe set expression using Bayesian *t*-tests with the R package “limma.” Principal component analysis (PCA) was performed based on RAT expression using the R package “FactoMineR.” Archetypal analysis (AA) was performed using the “archetypes” package.

AA is a method of unsupervised analysis that extrapolates a pre-defined *k* number of theoretical biopsies (archetypes, denoted by “A”) that represent the idealized phenotypes in a given data set. Each biopsy is then scored (denoted by “S”) to reflect its weighted distance from each *k* theoretical archetype such that the sum of scores is 1:

$$\sum_{i=1}^k S_i = 1$$

We performed AA on TBBs based on RAT expression and assigned TBBs to groups according to highest archetype score.

This study was approved the University of Alberta Research Ethics Board (Pro00048176) and the IRBs at participating centers. Written informed consent was received from patients before inclusion in this study.

Results

Patient and biopsy characteristics

We obtained 242 single-piece TBBs from 209 lung transplant recipients at 7 centers, with a second piece from 12 patients for studying sampling variation ([Table 1](#), see also [Table S2](#) online). TBB histology was interpreted as per SOC at the biopsying center. TBBs were done for clinical indications (e.g., decline in spirometry), follow-up, and

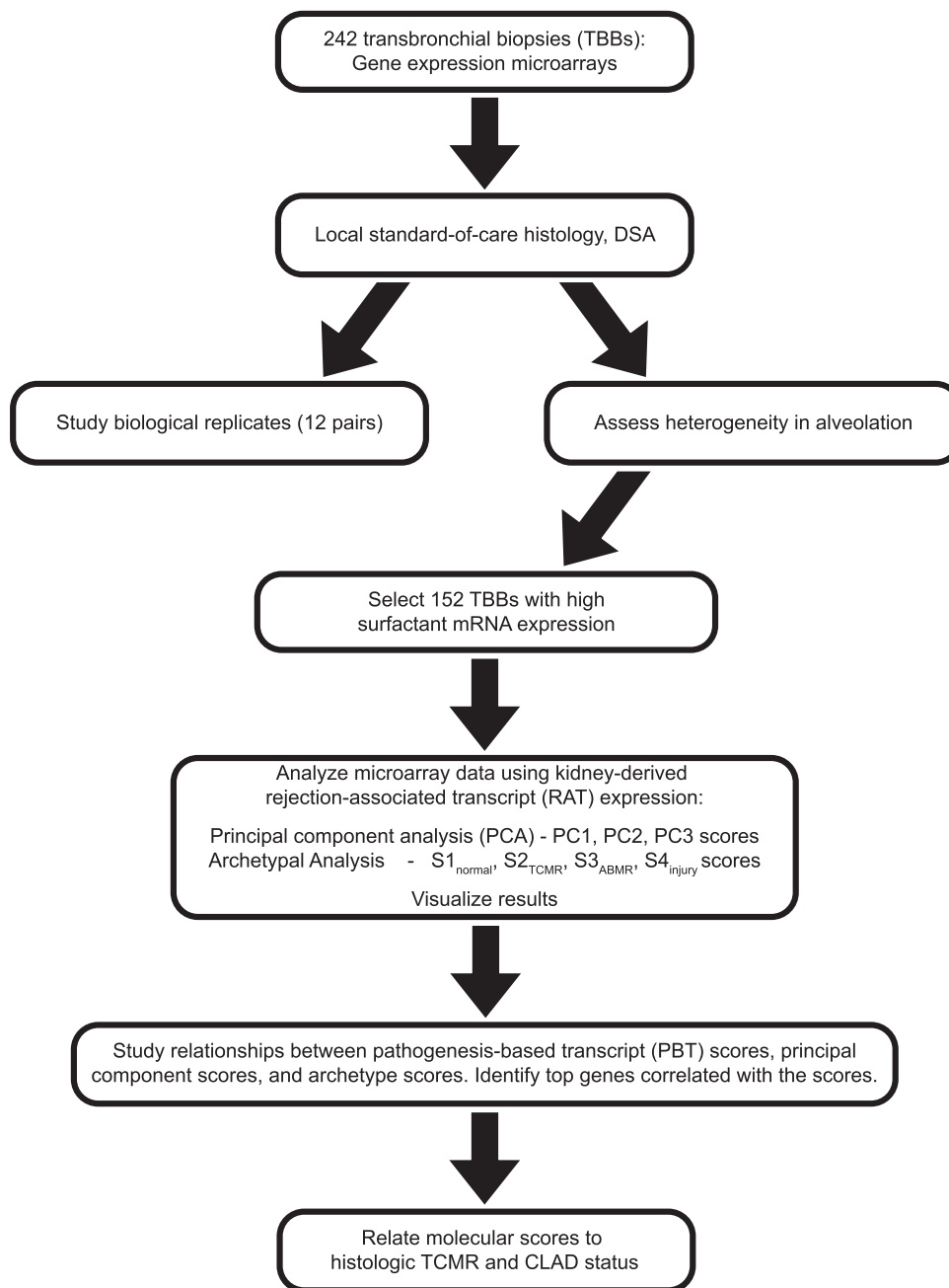


Figure 1 Study design for INTERLUNG.

protocol/surveillance; 69 biopsies (30% of tested patients) were from patients positive for DSA (Table 1). Most TBBs were done early post-transplant (median 256 days).

In 234 TBBs with available ISHLT grades, 144 were A0, 56 were A-grade ≥ 1 (i.e., ACR or TCMR), and 34 were ungradable (Ax), similar to previous studies.⁹ ISHLT B- and C-grade lesions could not be read in half of the TBBs and, of those that were gradable, only 9 were graded B ≥ 1 R and 6 C ≥ 1 , similar to previous studies,⁶ and 107 biopsies (46%) came from centers where C-grade assessment is not SOC. Thus, there were too few TBBs with B and C lesions to analyze these lesions' relationships with molecular states.

Overall pathology diagnoses were: ACR, 50 cases; antibody-mediated rejection (AMR), 12 cases; and mixed

rejection, 5 cases. There were 12 clinically diagnosed AMR cases, but only 5 of those were called AMR by histology, consistent with the known diagnostic uncertainty with respect to AMR in lung transplants.

Agreement between TBB pieces taken at the same time

In general, single-piece TBBs yielded high-quality RNA suitable for microarray analysis. In 12 cases where 2 TBB pieces were available from the same biopsy, we assessed agreement between the 2 pieces in terms of expression of PBTs representing biologic processes in rejection and injury (see Methods). In a permutation test of 1,000 iterations of random pairing, the true TBB pairs showed better

Table 1 INTERLUNG Transbronchial Biopsy Histologic Characteristics and Patient DSA Status

Biopsy characteristics	All TBBs (<i>N</i> = 242)	High surfactant TBBs (<i>N</i> = 152)
DSA at biopsy ^a (% of known)		
Positive	69 (30%)	46 (31%)
Negative	159 (70%)	103 (69%)
Not tested	14	3
Local pathology diagnosis ^b (% of known)		
ACR (TCMR)	55 (24%)	44 (29%)
AMR (ABMR)	17 (7%)	14 (9%)
Bronchiolitis obliterans	6 (3%)	4 (3%)
Lymphocytic bronchiolitis	6 (3%)	2 (1%)
Other	47 (20%)	36 (24%)
No findings	113 (49%)	66 (44%)
Indeterminate ^c	29 (13%)	16 (11%)
Not recorded	10	1
ISHLT A-grade (% of known)		
0	149 (62%)	88 (58%)
1	37 (15%)	29 (19%)
2	16 (7%)	12 (8%)
3 or 4	4 (2%)	3 (2%)
Ungradable (x)	36 (15%)	20 (13%)
Not recorded	0	0
ISHLT B-grade (% of known)		
0	118 (49%)	80 (52%)
1R or 2R	9 (4%)	4 (3%)
Ungradable (x)	115 (48%)	68 (45%)
Not recorded	0	0
ISHLT C-grade (% of known)		
0	25 (10%)	3 (2%)
1	6 (2%)	4 (3%)
Ungradable (x)	124 (51%)	71 (47%)
Not done ^d	87 (36%)	74 (49%)
Not recorded	0	0

^aThe most recent DSA status at time of recent biopsy was used, if known. DSA statuses dated more than 14 days after the biopsy were not considered. If the most recent DSA status at time of biopsy was not known, but the patient was most recently PRA negative, the DSA status was presumed negative. ACR, acute cellular rejection; AMR, antibody-mediated rejection; DSA, donor-specific antibody; ISHLT, International Society for Heart and Lung Transplantation; PRA, panel-reactive antibody; TBB, transbronchial biopsy; TCMR, T-cell-mediated rejection.

^bDiagnoses described by the local pathologist. Some samples had multiple diagnoses.

^cSamples were of insufficient quality to make a diagnosis based on histologic assessment (ungradable).

^dNot performed in the center's standard-of-care TBB assessment.

agreement in PBT scores than expected by chance ($p < 0.01$; see Figure S1 online), but with some variation in individual PBT scores between TBBs from the same patient.

TBB heterogeneity in alveolar content

Because alveolar content varies between single TBB pieces, we estimated alveolar content by identifying transcripts characteristic of alveoli. We compared gene expression in 242 TBBs with 34 biopsies from the mucosa at the second bronchial bifurcation (2BMB), which lack alveoli (Table 2). Most of the top differentially expressed transcripts were surfactant transcripts (SFTs), expressed up to 700 times more strongly in TBBs than 2BMBs.

We selected highly expressed SFTs to reflect alveolar content. Twenty-three TBBs (10%) had no SFTs (mean expression <100) and presumably lacked alveoli, and some

others had low SFTs (Figure 2). Alveolar content could affect endothelial transcript expression because alveoli contain more capillaries than non-alveolar tissues.²⁶

To reduce heterogeneity in alveolar content, we restricted the subsequent analyses to 152 TBBs with SFT expression level >12,380, the point where mean SFT expression dropped sharply (Figure 2). Lung function at biopsy (as measured by forced expiratory volume in 1 second [FEV₁]) did not differ significantly between the excluded biopsies and the 152 high-SFT biopsies ($p = 0.49$).

AA and PCA in 152 high-surfactant TBBs

Following the strategy successful for heart transplant biopsies,^{20,24} we used unsupervised AA based on RAT expression to derive the TBB archetype model. RAT performance

Table 2 Top Differentially Expressed Genes in TBB vs 2BMB ^a				
Probe set ID	Gene symbol	Gene title	Fold change TBB vs 2BMB	p-value ^b
11742494_s_at	<i>SFTPA1</i>	Surfactant protein A1	700	6×10^{-45}
11764024_x_at	<i>SFTPC</i>	Surfactant protein C	410	1×10^{-44}
11735664_s_at	<i>SFTPA2</i>	Surfactant protein A2	253	5×10^{-38}
11734773_x_at	<i>SFTPB</i>	Surfactant protein B	248	1×10^{-42}
11722312_a_at	<i>CLDN18</i>	Claudin 18	141	3×10^{-38}
11733543_at	<i>SFTA2</i>	Surfactant-associated 2	129	5×10^{-42}
11747224_s_at	<i>EDNRB / SFTPB</i>	Endothelin receptor type B/surfactant protein B	111	1×10^{-43}
11724148_at	<i>SFTPD</i>	Surfactant protein D	91	2×10^{-44}
11725436_a_at	<i>SCGB3A2</i>	Secretoglobin, family 3A, member 2	67	7×10^{-31}
11723949_a_at	<i>C4BPA</i>	Complement component 4-binding protein, alpha	61	3×10^{-45}

2BMB, second bronchial bifurcation mucosal biopsies; ID, identification; TBB, transbronchial biopsies.

^aBy fold change in 242 TBBs vs 34 2BMBs.

^bCalculated using two-tailed Bayesian *t*-tests.

was validated in the TBBs: ABMR RATs and TCMR RATs correlated opposingly with PC2, and Rejection RATs correlated with PC1 (Figure 3). The scree plot in Figure 4A illustrates how much variance is explained by adding additional archetypes to the model. Based on this and our experience with heart biopsies²⁴ we elected to use 4 archetypes, provisionally designated as A1 (normal), A2 (TCMR), A3 (ABMR-like, reflecting the uncertainty in conventional lung AMR diagnosis), and A4 (injury).^{20,24} As in hearts, we use “injury” to encompass all processes causing abnormal RAT expression uncorrelated with the rejection scores S2_{TCMR} and S3_{ABMR-like}. Each TBB was assigned 4

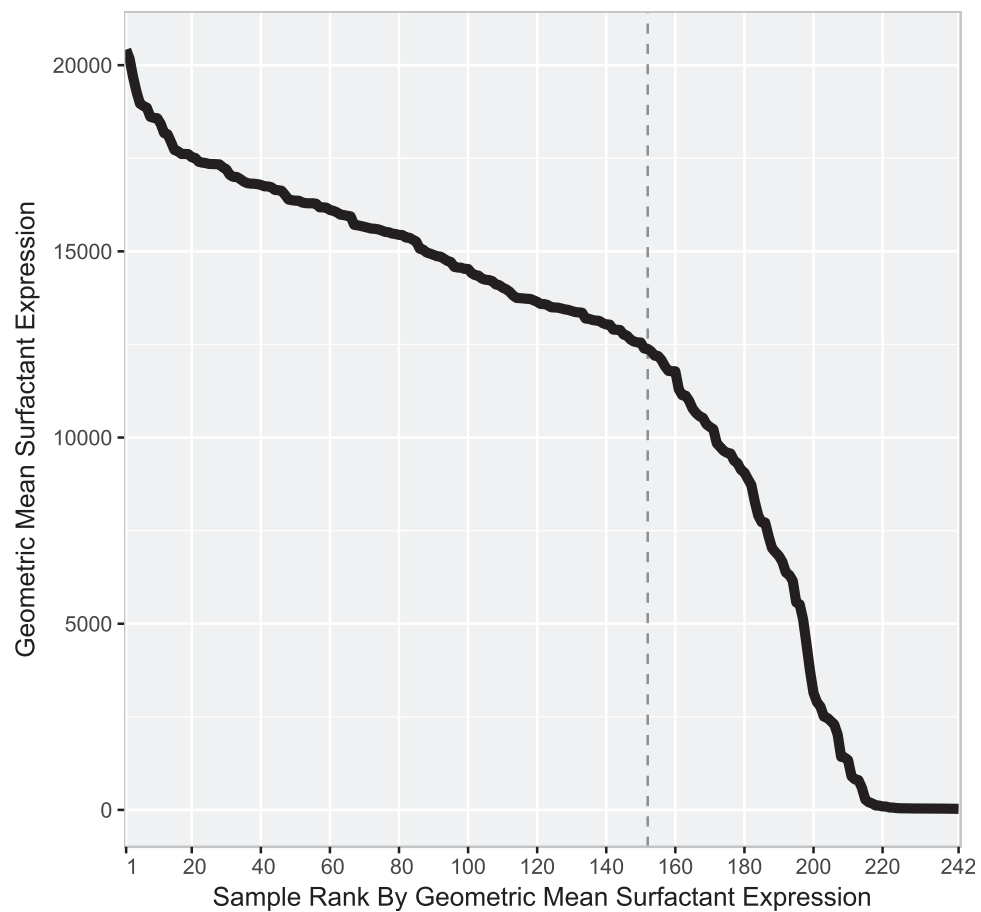


Figure 2 Surfactant (SFT) transcript expression in 242 TBBs. The 50 highest variance probe sets in 242 TBBs were identified. From this, 11 probe sets representing 4 SFT transcripts were identified (11757270_x_at, 11763961_x_at, 11754641_x_at, 11742494_s_at, 11735664_s_at, 11764024_x_at, 11748373_s_at, 11734773_x_at, 11745166_x_at, 11763809_x_at, 11749911_x_at) and their geometric mean expression across 242 TBB samples was calculated. The samples were ordered by decreasing geometric mean. The 152 samples to the left of the dashed vertical line were considered to have sufficiently high SFT expression (i.e., high alveolar content) to be used in subsequent analyses of the TBBs.

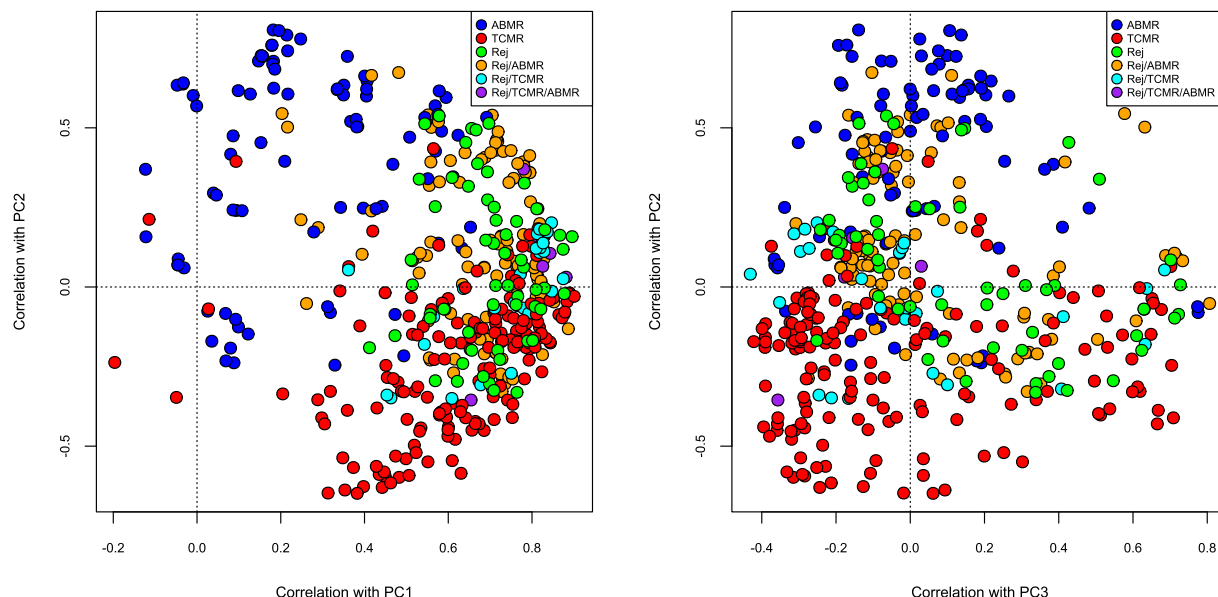


Figure 3 Correlations between RATs and the principal component scores in principal component analysis of 152 high-surfactant TBBs. The 453 RATs are the union of the top 200 transcripts associated with each of the following class comparisons in kidney transplant biopsies: all rejection (rej) vs everything else; TCMR vs everything else; and ABMR vs everything else. The transcripts are color-coded according to which of the 3 comparisons they were associated with.

corresponding scores ($S1_{\text{normal}}$, $S2_{\text{TCMR}}$, $S3_{\text{ABMR-like}}$, and $S4_{\text{injury}}$), reflecting its weighted similarity to each archetype.

TBBs were plotted in RAT-based PCA (Figure 4B–D), giving each biopsy linearly uncorrelated principal component scores (PC1, PC2, and PC3) that describe the principal sources of variation among the biopsies. TBBs were grouped and colored according to their highest AA score (Figure 4B–D). PC1 separated rejection and injury from normal (Figure 4B and D); PC2 separated ABMR-like TBBs from TCMR (Figure 4B and C); and PC3 separated injury from the rejection and normal groups (Figure 4C and D).

Correlation of AA and PCA scores with PBT expression

$S1_{\text{normal}}$ and PC1 demonstrated strong correlations with expression of all-rejection RATs, TCMR-RATs, and interferon-gamma (IFNG)-inducible transcripts (GRIT1s) (Figure 5). $S1_{\text{normal}}$ correlations were strongly negative, whereas PC1 correlations were strongly positive. $S2_{\text{TCMR}}$ correlated with cytotoxic T-cell transcripts (QCATs) and TCMR-RATs. $S3_{\text{ABMR-like}}$ and PC2 correlated with ABMR-associated transcript sets DSASTs, ENDATs, and ABMR-RATs. $S4_{\text{injury}}$ and PC3 correlated most strongly with macrophage transcripts (QCMATs), are associated with injury and depressed left ventricular fraction in heart transplants.²⁴

SFT expression did not correlate with endothelial and ABMR-related PBTs in TBBs with adequate alveoli, validating our strategy of limiting analyses to high-surfactant TBBs.

Top transcripts correlated with AA and PCA scores

Using RAT expression as the basis for PCA and archetype scores does not guarantee that RATs will be the dominant transcripts associated with these scores. The top 20 unique transcripts by absolute correlation with each score (out of 50,000 probe sets on the microarray) are summarized in terms of their expression in a human cell panel²⁷ in Table 3, and listed in Tables S3 through S6 (archetype scores) and Tables S7 through S9 (PCA scores) online. Thirteen of 20 $S1_{\text{normal}}$, 18 of 20 $S2_{\text{TCMR}}$, 2 of 20 $S3_{\text{ABMR-like}}$, 0 of 20 $S4_{\text{injury}}$, 15 of 20 PC1, 3 of 20 PC2, and 1 of 20 PC3 top associated transcripts were RATs. $S1_{\text{normal}}$ and PC1 anti-correlated and correlated, respectively, with inflammation; $S2_{\text{TCMR}}$ correlated with effector T-cell transcripts and certain macrophage transcripts (e.g., see ADAMDEC1 in Table S4 online); $S3_{\text{ABMR-like}}$ correlated with endothelial transcripts; and $S4$ correlated with macrophage transcripts. A full analysis of these relationships will be presented in a future study (manuscript in preparation).

Relating molecular scores to histologic TCMR

The only histologic diagnosis represented sufficiently in this TBB population for comparison with MMDx scores was A-grade histologic TCMR/ACR. Elevated $S2_{\text{TCMR}}$ scores were strongly associated with A ≥ 1 (one-tailed Mann–Whitney U -test, $p = 1 \times 10^{-5}$). High PC1 ($p = 1 \times 10^{-3}$) and low PC2 ($p = 8 \times 10^{-4}$) scores were also associated with A ≥ 1 . $S3_{\text{ABMR-like}}$, $S4_{\text{injury}}$, and PC3 were not significantly associated with A-grade ($p > 0.05$). There were not enough samples with positive B- or C-grades to assess relationships.

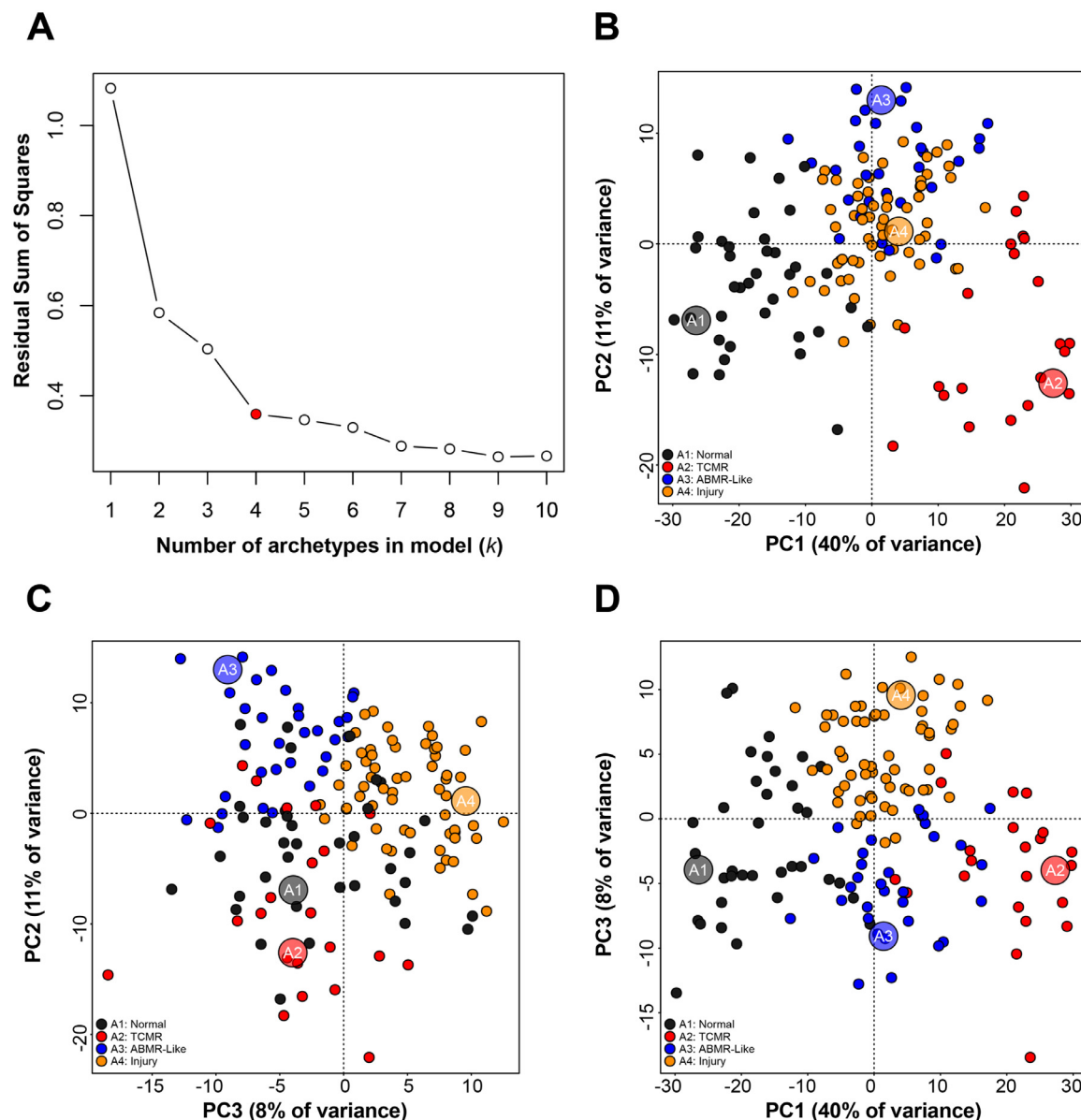


Figure 4 Archetypal analysis of 152 TBBs based on expression of rejection-associated transcripts (RATs). (A) Scree plot depicting residual sums of squares for archetypal analysis models built using different numbers of archetypes, k . In models with $k = 5$ through $k = 10$ archetypes, the relatively stable residual sum of squares suggests that little information is gained by examining more than 4 archetypes (red dot). Thus, the present study focuses on a 4-archetype model. (B–D) RAT-based archetypal analysis of 152 TBBs using 4 archetypes, visualized in RAT-based principal component analysis (PCA). (B) plots principal component 2 (PC2) vs PC1, (C) plots PC2 vs PC3, and (D) plots PC3 vs PC1. Each sample is colored according to its archetype cluster membership, which was determined by its highest of 4 archetype scores. The large ghosted points labeled “A1,” “A2,” “A3,” and “A4” denote the position of the theoretical archetypes in PCA.

As expected, given the low frequency of ABMR in this population, there were no associations between molecular scores and either clinical or histologic diagnoses of ABMR or with DSA at biopsy. A class comparison of biopsies from DSA-positive vs DSA-negative patients revealed no transcripts significantly associated with DSA positivity (data not shown).

Relationships between molecular scores and infection

Many biopsies came from patients recorded by the clinician as having some evidence for infection, but these were

highly heterogeneous and did not differ significantly between archetype groups (Chi-square test: any infection, $p = 0.33$; viral, $p = 0.60$; bacterial, $p = 0.40$; fungal, $p = 0.50$).

Discussion

This prospective discovery study of consented patients used unsupervised analysis based on RAT expression to identify molecular states in lung transplant TBBs. The goal was not a comprehensive diagnostic system, which would require a larger biopsy set, but rather an exploration of the feasibility and utility of using molecular approaches previously used

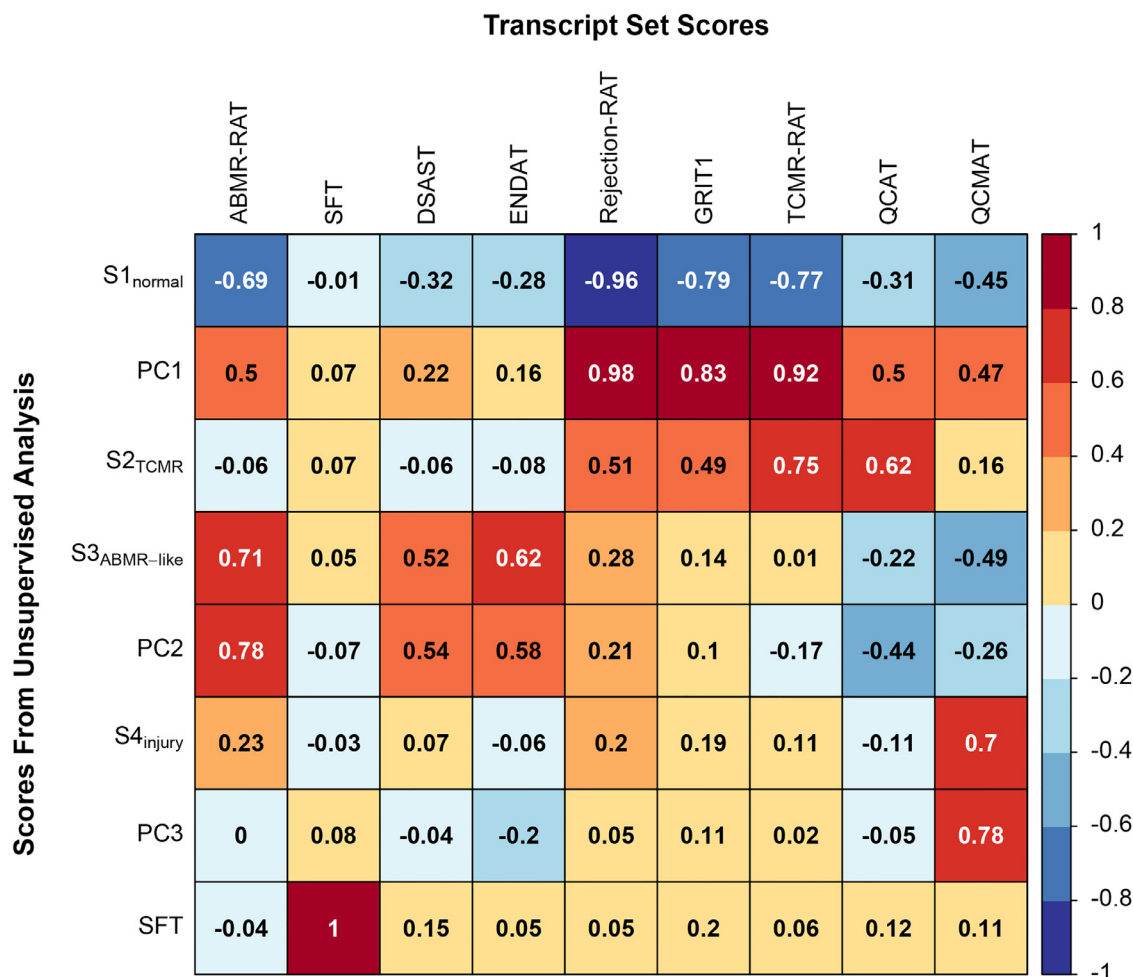


Figure 5 Correlations of molecular scores in 152 TBBs. Spearman correlations between molecular features of the samples are given and the cells are colored according to the magnitude of the correlation. Archetype scores (S1_{normal}, S2_{TCMR}, S3_{ABMR-like}, S4_{injury}) and principal component scores (PC1, PC2, PC3) were trained on RAT expression in 152 TBBs. QCAT, ENDAT, DSAST, QCMAT, and GRIT1 transcripts in the top 50% of expression variance in the full set of 242 TBBs were used. RATs were excluded from all other transcript sets. Column order is dictated by Ward's minimum variance clustering on a Manhattan distance matrix of the scores across 152 TBBs. ABMR-RAT, ABMR-associated RATs; TCMR-RAT, TCMR-associated RATs; Rejection-RAT, rejection-associated RATs; SFT, surfactant; DSAST, DSA-associated transcripts; ENDAT, endothelium-associated transcripts; QCMAT, macrophage-associated transcripts; QCAT, cytotoxic T-cell-associated transcripts; GRIT1, interferon-gamma-inducible transcripts.

for heart transplants, leveraging the sharing of molecular features of rejection and injury between organs in related disease processes, as previously demonstrated for heart²⁴

and kidney transplants.^{21,23,28} IRBs limited the study mainly to single-piece TBBs, forcing us to confront TBB composition heterogeneity. Every single-piece TBB

Table 3 Summary of Transcripts Associated With Archetype Scores and Principal Components

Score ^a	Key cellular expression patterns of the top 20 transcripts correlated or anti-correlated with the molecular score	Interpretation
S1 _{normal}	5 IFNG-inducible, 8 T/NK, 7 T/NK/MMDC	Absence of rejection and injury
S2 _{TCMR}	15 T (5 T, 5 T/NK, 5 T/NK/MMDC), 3 IFNG-inducible, 2 MMDC	T-cell-mediated rejection
S3 _{ABMR-like}	17 HUVEC, 1 T/NK/MMDC, 1 MMDC, 1 parenchymal	Endothelial
S4 _{injury}	19 MMDC (16 MMDC, 3 T/NK/MMDC), 1 HUVEC	Macrophage infiltration (injury)
PC1	7 IFNG-inducible, 6 T/NK, 7 T/NK/MMDC	Rejection/inflammation
PC2	10 HUVEC, 2 IFNG-inducible, 5 MMDC, 1 parenchymal, 2 unclear (low expression)	Endothelial
PC3	1 IFNG-inducible, 18 MMDC (14 MMDC, 4 T/NK/MMDC) 1 HUVEC	Macrophage infiltration (injury)

ABMR, antibody-mediated rejection; HUVEC, human umbilical vein endothelial cells; IFNG, interferon-gamma; MMDC, macrophages, monocytes, or dendritic cells; NK, natural killer cells; T, effector T cells; TCMR, T-cell-mediated rejection.

^a13 S1_{normal}, 18 S2_{TCMR}, 2 S3_{ABMR}, 0 S4_{injury}, 15 PC1, 3 PC2, and 1 of the PC3 top 20 transcripts were RATs.

produced high-quality readable RNA. Second TBB pieces available for 12 TBBs showed significant similarity in PBT expression, but with considerable variability. One source of variability was alveolar content, requiring that the analyses be restricted to 152 single-piece TBBs with high SFT expression. We performed unsupervised analyses of these TBBs to assign scores analogous to those used for heart transplants, and demonstrated the relationship between these scores and histologic TCMR as reflected by the A lesions, setting a framework for future clinical development of a definitive diagnostic system.

The $S2_{\text{TCMR}}$ score emerges as a reliable indicator of true TCMR, supported by its molecular similarity to TCMR in kidney and heart transplant biopsies and its association with histologic A-grade TCMR. For example, *ADAM-DEC1*, which encodes an enzyme expressed by activated macrophages, is highly associated with $S2_{\text{TCMR}}$ in lungs as well as with TCMR in kidney²⁷ and heart transplants (unpublished data). *ADAMDEC1* is not prominent in TBBs with high $S4_{\text{injury}}$ and PC3 scores, despite expression of many other macrophage transcripts. We believe that *ADAMDEC1* induction reflects a macrophage activation phenotype relatively specific for the cognate TCMR process in kidney, heart, and lung, reflecting interactions between effector T cells and macrophages, distinct from non-specific inflammation.

The relationship of $S3_{\text{ABMR-like}}$ scores to true ABMR, like many aspects of ABMR in lung transplants, remains elusive and will be resolved in future studies targeting ABMR. Given the paucity of ABMR in the current set of TBBs, our finding that neither $S3_{\text{ABMR-like}}$ scores nor individual transcripts correlate with DSA positivity was expected. The association of DSA with conventional lung transplant phenotypes has also been difficult to establish.²⁹

The non-rejection molecular changes that we designated injury—meaning all non-rejection sources of disturbance in RAT expression—are of particular interest in lung transplantation because of the many non-rejection-related stresses on lung tissue.³⁰ We first explored the molecular injury phenotype in kidney transplants, mapping transcripts (including some macrophage transcripts) associated with impaired function (glomerular filtration rate) in the absence of rejection.^{21,23,28,31} Histology did not reflect recent kidney injury.³¹ Similarly, the $S4_{\text{injury}}$ score in heart transplants correlated with impaired function (left ventricular ejection fraction).²⁴ In TBBs, like heart transplants, $S4_{\text{injury}}$ and PC3 were strongly associated with macrophage transcripts. Although we found no correlation between $S4_{\text{injury}}$ scores and FEV₁ in lungs, this issue will be of interest in future studies. Association of injury with macrophages does not exclude a role for neutrophils in lung injury: mRNA studies underestimate the role of neutrophils because they are unstable *in vitro* and cannot be included in cell panels. Moreover, granulocyte populations have abundant RNases that rapidly destroy their mRNA. Despite this, the top transcript associated with $S4_{\text{injury}}$ was neutrophil cytosolic factor 2 (*NCF2*), a transcript shared by neutrophils and macrophages. Pathway analysis also pointed to neutrophil involvement (data not shown). The role of neutrophils in

lung injury is of particular interest because lung tissue is characterized by high neutrophil influx compared with hearts or kidneys.³²

The ability to molecularly phenotype small pieces from TBB opens the possibility of establishing the mechanisms of CLAD and being able to predict its development. CLAD is difficult to study because of its variable presentation and lack of histologic definition, and also because it may involve lung compartments that are underrepresented in TBBs (e.g., small airways). The MMDx TBB approach can shed light on the role of rejection or related inflammatory mechanisms in CLAD.

A major advantage of the MMDx system is the assignment of continuous measurements with high technical reproducibility.³³ The significant similarity between single TBBs is encouraging evidence that they represent the biology of the lung, but the variability between single TBB pieces suggests that reliable MMDx diagnoses will require at least 2 pieces on 1 microarray. As algorithms mature with more samples, sampling variation (including alveolar content) may be reduced by incorporating a correction factor because we have been able to do this for the cortex–medulla issue in kidneys.³³

Our study has provided a definitive basis for the next steps in the discovery process: a new INTERLUNG study focusing on building the reference set with a particular focus on the molecular definition of ABMR and CLAD, which will require long-term follow-up. Our results support our request to IRBs to permit 2 TBB pieces per biopsy to offset sampling heterogeneity. Ultimately, our goal is to develop a reference set of at least 1,000 TBBs and to relate the findings to clinical phenotypes, effects of treatment, and prognosis. This will allow us to derive a set of RATs in the TBBs, which will in turn permit us to validate the use of kidney RATs in the analysis of lung rejection; compare the lung, heart, and kidney transcripts; and potentially identify molecular processes that may be unique to rejection in lung tissue. In parallel, we are now in the process of exploring the utility of bronchial mucosal biopsies, a safer biopsy format (ClinicalTrials.gov [NCT02812290](https://clinicaltrials.gov/ct2/show/study?term=NCT02812290)).³⁴

Disclosure statement

P.F.H. holds shares in Transcriptome Sciences, Inc., a University of Alberta research company with an interest in molecular diagnostics. The remaining authors have no conflicts of interest to disclose.

This research was supported by funds and/or resources from the Mendez National Institute of Transplantation Foundation, Roche Organ Transplant Research Foundation, and the University of Alberta Hospital Foundation.

The authors are grateful to Drs. Justin Weinkauff, Dale Lien, Ali Kapasi, and Alim Hirji for providing biopsy specimens.

Portions of this study were presented at the 38th annual meeting and scientific sessions of the International Society for Heart and Lung Transplantation, April 12, 2018, Nice, France.

Supplementary data

Supplementary data associated with this article can be found in the online version at www.jhltonline.org/.

References

- Yusen RD, Edwards LB, Kucheryavaya AY, et al. The Registry of the International Society for Heart and Lung Transplantation: Thirty-second official adult lung and heart–lung transplantation report—2015; Focus theme: Early graft failure. *J Heart Lung Transplant* 2015;34:1264–77.
- Todd JL, Christie JD, Palmer SM. Update in lung transplantation 2013. *Am J Respir Crit Care Med* 2014;190:19–24.
- Stewart S, Fishbein MC, Snell GI, et al. Revision of the 1996 working formulation for the standardization of nomenclature in the diagnosis of lung rejection. *J Heart Lung Transplant* 2007;26:1229–42.
- Faro A, Visner G. The use of multiple transbronchial biopsies as the standard approach to evaluate lung allograft rejection. *Pediatr Transplant* 2004;8:322–8.
- Trulock EP. The role of transbronchial lung biopsy in the treatment of lung transplant recipients. An analysis of 200 consecutive procedures. *Chest* 1992;102:1049.
- Chamberlain D, Maurer J, Chapparro C, Idolor L. Evaluation of transbronchial lung biopsy specimens in the diagnosis of bronchiolitis obliterans after lung transplantation. *J Heart Lung Transplant* 1994;13:963–71.
- Burton CM, Iversen M, Scheike T, Carlsen J, Andersen CB. Is lymphocytic bronchiolitis a marker of acute rejection? An analysis of 2,697 transbronchial biopsies after lung transplantation. *J Heart Lung Transplant* 2008;27:1128–34.
- Glanville AR, Aboyoun CL, Havryk A, Plit M, Rainer S, Malouf MA. Severity of lymphocytic bronchiolitis predicts long-term outcome after lung transplantation. *Am J Respir Crit Care Med* 2008;177:1033–40.
- Arcasoy SM, Berry G, Marboe CC, et al. Pathologic interpretation of transbronchial biopsy for acute rejection of lung allograft is highly variable. *Am J Transplant* 2011;11:320–8.
- Valentine VG, Gupta M, Weill D, et al. Single-institution study evaluating the utility of surveillance bronchoscopy after lung transplantation. *J Heart Lung Transplant* 2009;28:14–20.
- McWilliams TJ, Willam C, Whitford HM, Snell GI. surveillance bronchoscopy in lung transplant recipients: risk versus benefit. *J Heart Lung Transplant* 2008;27:1203–9.
- Sandrini A, Glanville A. The controversial role of surveillance bronchoscopy after lung transplantation. *Curr Opin Organ Transplant* 2009;14:494–8.
- Berry G, Burke M, Andersen C, et al. Pathology of pulmonary antibody-mediated rejection: 2012 update from the Pathology Council of the ISHLT. *J Heart Lung Transplant* 2013;32:14–21.
- Levine DJ, Glanville AR, Aboyoun CL, et al. Antibody-mediated rejection of the lung: a consensus report of the International Society for Heart and Lung Transplantation. *J Heart Lung Transplant* 2016;35:397–406.
- Camacho DM, Collins KM, Powers RK, Costello JC, Collins JJ. Next-generation machine learning for biological networks. *Cell* 2018;173:1581–92.
- Sellares J, Reeve J, Loupy A, et al. Molecular diagnosis of antibody-mediated rejection in human kidney transplants. *Am J Transplant* 2013;13:971–83.
- Reeve J, Sellares J, Mengel M, et al. Molecular diagnosis of T cell-mediated rejection in human kidney transplant biopsies. *Am J Transplant* 2013;13:645–55.
- Mueller TF, Einecke G, Reeve J, et al. Microarray analysis of rejection in human kidney transplants using pathogenesis-based transcript sets. *Am J Transplant* 2007;7:2712–22.
- Halloran PF, Famulski KS, Reeve J. Molecular assessment of disease states in kidney transplant biopsy samples. *Nat Rev Nephrol* 2016;12:534–48.
- Halloran PF, Potena L, Duong Van Huyen JP, et al. Building a tissue-based molecular diagnostic system in heart transplant rejection: the heart molecular microscope MMDx. *J Heart Lung Transplant* 2017;36:1192–200.
- Halloran PF, Venner JM, Famulski KS. Comprehensive analysis of transcript changes associated with allograft rejection: combining universal and selective features. *Am J Transplant* 2017;17:1754–69.
- Halloran PF, Akalin E, Aubert O, et al. Real time central assessment of kidney transplant indication biopsies by microarrays: the INTERCOMEX study. *Am J Transplant* 2017;17:2851–62.
- Halloran PF, Venner JM, Madill-Thomsen K, et al. Review: The transcripts associated with organ allograft rejection. *Am J Transplant* 2018;18:785–95.
- Halloran PF, Aliabadi AZ, Bruneval P, et al. Exploring the cardiac response-to-injury in heart transplant biopsies. *JCI Insight* 2018;3:e123674.
- Reeve J, Einecke G, Mengel M, et al. Diagnosing rejection in renal transplants: a comparison of molecular- and histopathology-based approaches. *Am J Transplant* 2009;9:1802–10.
- Townsend MI. Structure and composition of pulmonary arteries, capillaries, and veins. *Compr Physiol* 2012;2:675–709.
- Venner JM, Famulski K, Badr D, Hidalgo LG, Chang J, Halloran PF. Molecular landscape of T cell-mediated rejection in human kidney transplants: prominence of CTLA4 and PD ligands. *Am J Transplant* 2014;14:2565–76.
- Famulski KS, Reeve J, de Freitas DG, Kreepala C, Chang J, Halloran PF. Kidney transplants with progressing chronic kidney diseases express high levels of acute kidney injury transcripts. *Am J Transplant* 2013;13:634–44.
- Hachem RR, Kamoun M, Budev MM, et al. Human leukocyte antigens antibodies after lung transplantation: primary results of the HALT Study. *Am J Transplant* 2018;18:2285–94.
- Gardner A, Borthwick LA, Fisher AJ. Lung epithelial wound healing in health and disease. *Expert Rev Respir Med* 2010;4:647–60.
- Famulski KS, de Freitas DG, Kreepala C, et al. Molecular phenotypes of acute kidney injury in human kidney transplants. *JASN* 2012;23:948–58.
- Scozzi D, Ibrahim M, Menna C, Krupnick AS, Kreisel D, Gelman AE. The role of neutrophils in transplanted organs. *Am J Transplant* 2017;17:328–35.
- Madill-Thomsen KS, Wiggins RC, Eskandary F, Bohmig GA, Halloran PF. The effect of cortex/medulla proportions on molecular diagnoses in kidney transplant biopsies: rejection and injury can be assessed in medulla. *Am J Transplant* 2017;17:2117–28.
- Halloran KM, Parkes MD, Chang J, et al. Molecular detection of rejection—like changes in proximal bronchial mucosal lung transplant biopsies: initial findings of the INTERLUNG study [abstract]. *J Heart Lung Transplant* 2018;37(suppl):S80–1.